Journal of Mechatronics, Electrical Power, and Vehicular Technology 15 (2024) 93-104

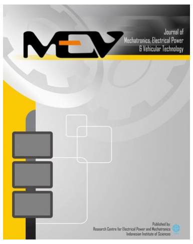

Journal of Mechatronics, Electrical Power, and Vehicular Technology

e-ISSN: 2088-6985
p-ISSN: 2087-3379

mev.brin.go.id

Robust remaining useful life prediction of lithium-ion battery with convolutional denoising autoencoder

Asri Rizki Yuliani [a, *], Hilman Ferdinandus Pardede [a], Ade Ramdan [a], Vicky Zilvan [a], Raden Sandra Yuwana [a], M Faizal Amri [b], R. Budiarianto Suryo Kusumo [a, c], Subrata Pramanik [d]

[a] *Research Center for Artificial Intelligence and Cyber Security, National Research and Innovation Agency*
Kawasan Sains dan Teknologi (KST) Samaun Samadikun, Jalan Sangkuriang, Bandung, 40135, Indonesia

[b] *Research Center for Smart Mechatronics, National Research and Innovation Agency*
Kawasan Sains dan Teknologi (KST) Samaun Samadikun, Jalan Sangkuriang, Bandung, 40135, Indonesia

[c] *Faculty of Electrical Engineering and Information Technology, Technische Universität Chemnitz*
Straße der Nationen 62, Chemnitz, D-09111, Germany

[d] *Faculty of Engineering, Rajshahi University*
Motihar, Rajshahi, 6205, Bangladesh

Abstract

Using lithium-ion (Li-ion) batteries exceeding their useful lifetime may be dangerous for users, and hence, developing an accurate prediction system for batteries that remain useful for life is necessary. Many deep learning models, such as gated recurrent units and long short-term memory (LSTM), have been proposed for that purpose and have shown good results. However, their performance when dealing with noisy data degrades significantly. This may hamper their implementations for the real world since battery data are prone to noise. In this paper, we develop a robust prediction model in a noisy environment for predicting the remaining useful life (RUL) of Li-ion batteries. We propose a denoising autoencoder (DAE) utilized to remove noise from the data. The DAE is built with convolutional layers instead of traditional feed-forward networks here. We combine DAE with LSTM as the predictor. The proposed framework is evaluated using artificially corrupted battery data provided by National Aeronautics and Space Administration (NASA). The results reveal that our proposed method improves robustness when data contain various types of noise. A comparative study using the traditional approach has also been conducted. Our evaluation shows that convolutional layers are more effective than the traditional approach and that the original composition of the DAE was built using traditional feed-forward networks. DAE with convolutional layers has the best average performance with MSE of 0.61 and is the most consistent model.

Keywords: denoising autoencoder (DAE); lithium-ion (Li-ion) battery; neural network; remaining useful life (RUL); system robustness.

* Corresponding Author. asri005@brin.go.id (A. R. Yuliani)

https://doi.org/10.55981/j.mev.2024.905

Received 28 May 2024; revised 16 July 2024; accepted 17 July 2024; available online 31 July 2024

How to Cite: A. R. Yuliani, *et al.*, "Robust remaining useful life prediction of lithium-ion battery with convolutional denoising autoencoder," *Journal of Mechatronics, Electrical Power, and Vehicular Technology*, vol. 15, no. 1, pp. 93-104, July, 2024.

I. Introduction

Lithium-ion (Li-ion) batteries are used in many electric devices, such as electric vehicles, smartphones, laptops, and power tools. They are popular due to their lightweight design, compact size, high energy density, rechargeability, and relatively long cycle life. However, using Li-ion batteries exceeding their useful life period is not recommended since it may lead to system malfunctions and even severe accidents. The unscheduled maintenance can result in a shorter battery lifespan and the need for more frequent replacements. Therefore, it is crucial to develop an accurate prediction system for the battery's remaining useful life (RUL) to ensure the service life of the battery and the safety of the application. One indicator of the age of these batteries is the discharge capacity. When this capacity decreases to 70 % - 80 % of the initial capacity, it signifies the end-of-life (EoL). So, the capacity prediction value can be used for assessing RUL [1].

Numerous studies for RUL prediction have been reported in the literature. We can group the approaches for RUL predictions into two. They are model-based approaches and data-driven approaches. Model-based approaches involve predicting the health condition of a system by building physical models. Since the system degradation process has stochastic behavior, these approaches can effectively predict battery deterioration. Markov process [2], the Wiener process [3], and Gaussian mixtures [4] are several examples of this category. However, these methods assume a stationary process for the data. Unfortunately, the battery data are non-stationary. To overcome this, various non-linear filters, such as particle filter (PF) or Kalman filter (KF) [5][6] are used instead. However, model-based approaches rely on in-depth understanding and domain expertise to develop suitable models for a specific battery. They usually have poor generalization capability to other systems, making them less practical to develop.

For data-driven approaches, the degradation process is modeled from past data. These approaches do not require explicit physical models; instead, they develop the model based on generic models that would be optimized to fit the data by optimizing the model's parameters and hyperparameters. When enough data are available, data-driven methods can be modified for many systems without very deep, pre-existing knowledge about the systems. For this, various machine learning methods, including deep learning [7], support vector regression (SVR) [8], and autoregressive moving average models (ARIMA) [9], are several popular machine learning techniques used in data-driven approaches. Recently, deep learning has received increasing attention in the RUL prediction of Li-ion batteries because of its ability to model non-linearities. Various architectures, such as convolution neural network (CNN) [10], long short-term memory (LSTM) [11][12], bidirectional LSTM (BiLSTM) [13], gated recurrent units (GRU) [14][15], and Transformers [16] have shown good performance for RUL prediction. Despite its popularity, one significant drawback still exists: producing a well-trained RUL predictor relies heavily on a large quantity of data. In other words, if the data selection is not sufficiently representative, the prediction performance can be highly unsatisfactory.

In addition to the quantity of the data, their quality is also essential. Usually, deep learning models are trained with clean data, so the distortions are minimal. Unfortunately, data in real environments usually contains distortions from noises and measurement errors. Therefore, there may be a mismatch between training and testing conditions, making the models prone to wrong predictions when used with noisy data and degrading their performance. The Li-ion battery itself has inherent characteristics of being non-linear, complex, and subject to dynamic changes; thus, the degradation curve typically follows non-linear and non-stationary patterns. Furthermore, data collected in a real environment often encounter missing values. Therefore, many deep learning models fail to achieve satisfactory performance [17][18].

To minimize this effect, a data preprocessing technique is required to enhance data quality. Some studies have implemented denoising filters, such as particle filters [5], to the data before applying the machine learning models. In [19], a hybrid filtering method combining unscented Kalman filter (UKF) with kernel adaptive filter (KAF)-based model is proposed to produce a more robust and reliable prediction model. A hybrid of denoising-prediction with empirical mode decomposition (EMD) is proposed in [20]. Complete ensemble empirical mode decomposition with adaptive noise (CEEMDAN) is used in front of LSTM classifiers in [21].

Deep learning can also be employed for noise reduction. One of them is the denoising autoencoder (DAE). In [22], a method combining DAE and GRU estimates the battery's state of charge (SoC). The DAE was utilized to achieve a robust SoC estimation by introducing noise during the network training process, which helps in extracting valuable feature data from corrupted input data. Moreover, in [23], a combined stacked DAE and feed-forward networks is proposed for temperature forecasting and electric power consumption. DAE for noise suppression in processing seismic data is proposed in [24]. DAE was initially

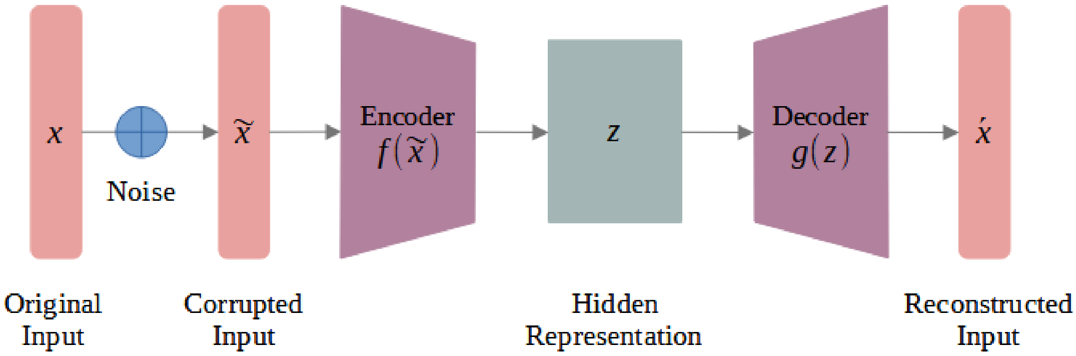

Figure 1. Architecture of DAE.

trained in a supervised manner using synthetic data, and then the pre-trained model was applied to denoise the field seismic data in an unsupervised manner. A sequence-to-sequence mapping based on the LSTM model for robust SoC estimation that employed DAE is proposed in [25]. A two-stage pretraining approach is adopted to improve the feature learning capability and make it robust against variable sampling frequency. In addition, DAE has been widely adopted in speech data [26] and time-series data [22][23][24].

In this paper, we proposed DAE for noise reduction of battery data. Here, we use convolutional layers instead of feed-forward layers for DAE to reduce the computational load and storage. We employ LSTM on top of DAE as a predictor. In this paper, we denote our hybrid architectures as DAE-LSTM. The contributions of this paper are summarized as follows. The proposed method uses the DAE to reduce noise in the data. For practical application, the RUL prediction system should be robust against noise. To our knowledge, very few studies employ DAE-LSTM for battery data. The proposed framework is evaluated using four artificially corrupted battery data provided by National Aeronautics and Space Administration (NASA). The experimental results show that the proposed DAE improves robustness when data contain various types of noise. A comparative study using a traditional approach named CEEMDAN was conducted. Specifically, we explore various configurations of DAE from the depth and the types of networks. Both feed-forward networks-based DAE and convolutional layer-based DAE are investigated. While initially intended for image data, we found that convolutional layer-based DAE is generally better than the original DAE. It is also generally better than CEEMDAN [21], which is employed with LSTM.

The remainder of this paper is organized as follows. Section II introduces the network architecture of the proposed method. Section II also describes the battery datasets, the process of adding noise, and the performance evaluation criteria. Section III gives the DAE's estimation performance and compares RUL prediction results with other methods. Finally, the concluding remarks are presented in Section IV.

II. Materials and Methods

A. Denoising autoencoder

An autoencoder is a neural network that compresses data using the encoder and reconstructs the data with the decoder components. The encoder maps the input features into a reduced representation vector to find their latent variables, while the decoder reconstructs the output features back into the original size. DAE is a variant of autoencoder that aims to learn robust data representation [27]. It is done by mapping the distorted data with their clean ones. So, DAE is trained to produce a denoised version of data given corrupted input [28].

As in the autoencoder, DAE consists of two components as well. They are encoder and decoder networks. Figure 1 shows the architecture of DAE. The original input x is first corrupted with noise. After that, the corrupted input $\tilde{x}$ is converted using the encoder network $f(\tilde{x}) = \sigma(W\tilde{x} + b)$ into a hidden representation z, where $\sigma(\cdot)$ is a non-linear activation function. W is a weight matrix, and b is a bias vector, which are the parameters of the network. Then, the resulting representation z is converted back using the decoder network $g(z) = \sigma(Wz + b)$ in an attempt to reconstruct the denoised version of the corrupted data $\acute{x}$. The decoder network mirrors the structure of the encoder network but in reverse order. DAE is trained by minimizing the error between the clean input x and its reconstructed input $\acute{x}$. In such a manner, DAE learns to eliminate undesirable noise from the data.

B. Proposed method

The proposed robust battery RUL prediction comprises two parts: DAE as the denoising model and LSTM as the prediction model. Here, we use DAE as preprocessing to eliminate noise from the data. DAE is

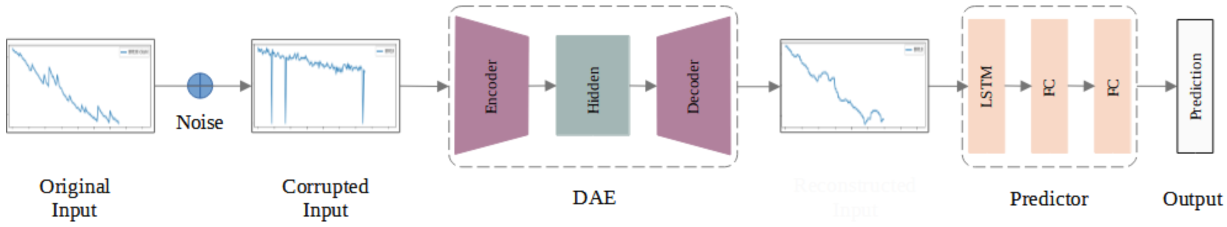

Figure 2. Architecture of the proposed system.

designed to take corrupted data as input and is trained to generate a prediction of the uncorrupted data as its output. For the prediction model, we use LSTM. The overview of our proposed system is depicted in Figure 2.

The proposed DAE is defined as follows. First, the original input is corrupted with noise. There are several ways to corrupt the input, such as adding Gaussian noise to the entire signal or only part of the signal or setting a desired proportion of the input values to zero at random. After that, the corrupted data are passed through the DAE network as the input layer. Secondly, the encoder network converts the corrupted input into a latent representation. The output size of the encoder is set to be smaller than the input size. We applied more than one non-linear encoding stage. Then, the decoder network reconstructs the output data given by hidden representation. The size of the hidden representation is converted back to the original input size. For example, in the encoding stage, we also applied more than one non-linear decoding stage. So, the decoder output is a denoised version of corrupted data that would be the input for the RUL prediction model. The output is the same size as the original input. When calculating the mean square error (MSE) as a loss function, the output is compared with the original clean input.

In this study, we employed two types of network architecture to build DAE. The first uses a fully connected network (FC), and the second uses a convolutional neural network (CNN). Here, we denote DAE for the first and CNNDAE for the latter. We consider using CNN as they are capable of modeling local relations between data. So, for battery data, CNN would emphasize data near time indices more. So, we expect CNN to learn effectively the trend pattern in the time series data. Other studies have also indicated similar observations. In addition to the network types, we also explore the depth of the networks. It is known that deeper networks enable better learning of more complex relationships [29]. We investigate DAE and CNNDAE architecture with different levels of depth of the hidden layer. For DAE, FC layers are adopted in the encoder and decoder networks. Meanwhile, CNNDAE comprises one-dimensional strided convolutional layers in the encoder and decoder networks. We denote DAE-1, DAE-2, and DAE-3 for the DAE model and CNNDAE-1, CNNDAE-2, and CNNDAE-3 for the CNNDAE model to indicate the number of hidden layers from one to three for each encoder and decoder. The detailed architectures of the proposed method are shown in Table 1. Feed-forward networks or fully connected networks are denoted as Dense in Table 1.

C. LSTM predictor

We applied the LSTM network for the prediction model. LSTM has gained extensive use in battery RUL prediction systems due to its ability to effectively capture long-term dependencies in time series data [30][31]. A common LSTM unit is composed of a cell and three gates. The gates are an input gate, an output gate, and a forget gate. Each gate has a distinctive task in controlling the flow of information into and out of the cell state. The prediction model consists of a single LSTM layer comprising 32 hidden units, followed by two FC layers. The detailed architecture of the predictor is shown in Table 2. This LSTM predictor architecture is used for all the proposed denoising methods.

D. Experimental data

The battery data set provided by NASA's Prognostic Center of Excellence (PCoE) is adopted to evaluate the reliability of the proposed method. We focus on four batteries designated as B5, B6, B7, and B18. These batteries underwent cycling until their capacity degraded to 70 % of their initial capacity. The cycling experiments were tested at room temperature and involved three operational profiles: charge, discharge, and impedance. Under the discharge measurement profile, the capacity degradation process for each battery is illustrated in Figure 3. The starting capacity of these four batteries is 1.86 Ah, 2.04 Ah, 1.89 Ah, and 1.86 Ah, respectively. Despite minor variations in their cyclic discharge conditions, their rated capacity is considered to be 2 Ah. Thus, the failure threshold is set to 1.4 Ah when the batteries drop 30 % of their rated capacity.

It is important to emphasize that the NASA battery dataset is collected under tightly controlled laboratory conditions. Thus, it is contaminated with minimal noise. In order to simulate the real working conditions, we introduced artificial noise to the original capacity

Table 1.
Architectures of the proposed DAE.

Model	Sub-network	Layer (configurations)	Output size	# Params
DAE-1	Encoder	InputLayer	20 × 1	0
		Dense (10, Tanh)	10 × 1	210
	Decoder	Dense (20, Linear)	20 × 1	220
DAE-2	Encoder	InputLayer	20 × 1	0
		Dense (10, Tanh)	10 × 1	210
		Dense (5, Tanh)	5 × 1	55
	Decoder	Dense (10, Tanh)	10 × 1	60
		Dense (20, Linear)	20 × 1	220
DAE-3	Encoder	InputLayer	20 × 1	0
		Dense (10, Tanh)	10 × 1	210
		Dense (5, Tanh)	5 × 1	55
		Dense (1, Tanh)	1 × 1	6
	Decoder	Dense (5, Tanh)	5 × 1	10
		Dense (10, Tanh)	10 × 1	60
		Dense (20, Linear)	20 × 1	220
CNNDAE-1	Encoder	InputLayer	20 × 1	0
		Conv1D (Tanh, Filter=10, Kernel=1)	20 × 10	20
		MaxPooling1D (Pool size=2)	10 × 10	0
	Decoder	UpSampling1D (Size=2)	20 × 10	0
		Conv1D (Linear, Filter=1, Kernel=11)	20 × 1	111
CNNDAE-2	Encoder	InputLayer	20 × 1	0
		Conv1D (Tanh, Filter=5, Kernel=1)	20 × 5	10
		Maxpooling1D (Pool size=2)	10 × 5	0
		Conv1D (Tanh, Filter=10, Kernel=3)	10 × 10	160
		Maxpooling1D (Pool size=2)	5 × 10	0
	Decoder	UpSampling1D (Size=2)	10 × 10	0
		Conv1D (Tanh, Filter=5, Kernel=1)	10 × 5	55
		UpSampling1D (Size=2)	20 × 5	0
		Conv1D (Linear, Filter=1, Kernel=3)	20 × 1	16
CNNDAE-3	Encoder	InputLayer	20 × 1	0
		Conv1D (Tanh, Filter=5, Kernel=1)	20 × 5	10
		Maxpooling1D (Pool size=2)	10 × 5	0
		Conv1D (Tanh, Filter=10, Kernel=3)	10 × 10	160
		Maxpooling1D (Pool size=2)	5 × 10	0
		Conv1D (Tanh, Filter=5, Kernel=1)	5 × 5	55
	Decoder	UpSampling1D (Size=2)	10 × 5	0
		Conv1D (Tanh, Filter=10, Kernel=1)	10 × 10	60
		UpSampling1D (Size=2)	20 × 10	0
		Conv1D (Tanh, Filter=5, Kernel=3)	20 × 5	155
		Conv1D (Linear, Filter=1, Kernel=1)	20 × 1	6

data. In realistic usage, batteries are usually used in an environment with variability, and their degradation behavior may be affected by fluctuations and measurement inaccuracies. Therefore, we introduced two types of noise: additive Gaussian noise and masking noise. The noise function is defined as in equation (1),

$$N(x) = \left(x + \mathcal{N}(\mu, \sigma^2)\right) .* B(n, p) \tag{1}$$

where $N(x)$ is the noisy version of the original battery data x of size n. $N(\cdot)$ is Gaussian noise sampled from Normal distribution with mean and variance settings. $B(\cdot)$ is masking noise sampled from Binomial distribution with probability p of being zero (masked).

Table 2.
Architecture of the LSTM predictor.

Layer	Output size	# Params
InputLayer	5 × 1	0
LSTM	32	4352
Dense	32	1056
Dense	1	33

The operator .* indicates an element-wise multiplication. In this experiment, we implement three scenarios:

- Gaussian noise only, where the probability of being masked is 0.
- Masking noise only, where Gaussian variance is 0
- Mixture noise.

Noise is introduced into the original capacity data to measure the robustness of the battery RUL prediction system. The resulting corrupted data, denoted as $N(x)$, is subsequently used in both the training and testing phases of the system. For training data, we used Gaussian noise with zero-mean and variance $\sigma^2 = [0.01,0.05,0.1]$, and masking noise percentage $p = [0.0,0.02,0.04,0.1]$. For test data, we utilized noises equivalent to noises in the training data with different parameter settings: Gaussian noise with zero-mean and variance $\sigma^2 = [0.0,0.01,0.05,0.1]$, and masking noise with $p = 0.03$. In addition, we added Gaussian noise with variance $\sigma^2 = [0.05,0.1,0.2,0.5]$ to part of the signal by 2 % in the test data. Figure 4 shows some examples of each generated artificial noisy data of battery B18.

In this experiment, we adopted the leave-one-out cross-validation technique, where one battery is designated as the test data, and the remaining three batteries serve as the training data. This process is repeated four times for each test set; the results shown are the average of these experiments. B5, B6, and B7 have similar degradation patterns and the same number of cycles; thus, we have chosen to display the graphical experimental results of batteries B5 and B18 only.

E. Experimental setup

For training the DAE, the hyperparameters are configured as follows. The entire model is trained with a sequence length of 20 and a 50 % overlap, with 50 epochs and a batch size of 8. During testing, there is no overlap in the sequence length. We used the Tanh activation function, and for optimization, we used the Adam optimizer with a learning rate of 10^{-3}. The detailed configurations of the proposed DAE are shown in Table 1. All the proposed DAE models are trained and tested using corrupted data with different noise parameter settings, as discussed in Section II.D.

The hyperparameters are set as follows to train the LSTM predictor. We used the Adam optimizer with a learning rate of 10^{-3}. We set the training epochs to 100, the batch size to 50, and the sequence length to 5. At

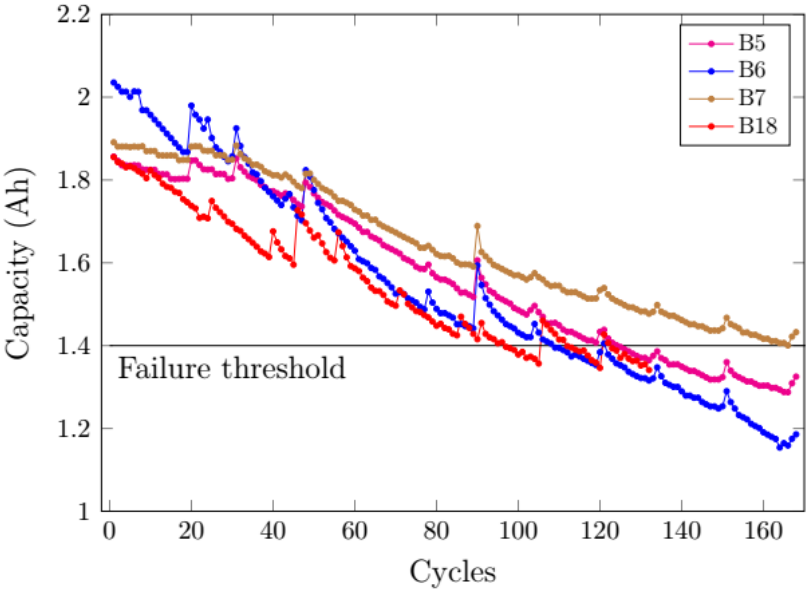

Figure 3. Capacity degradation over the discharging cycle.

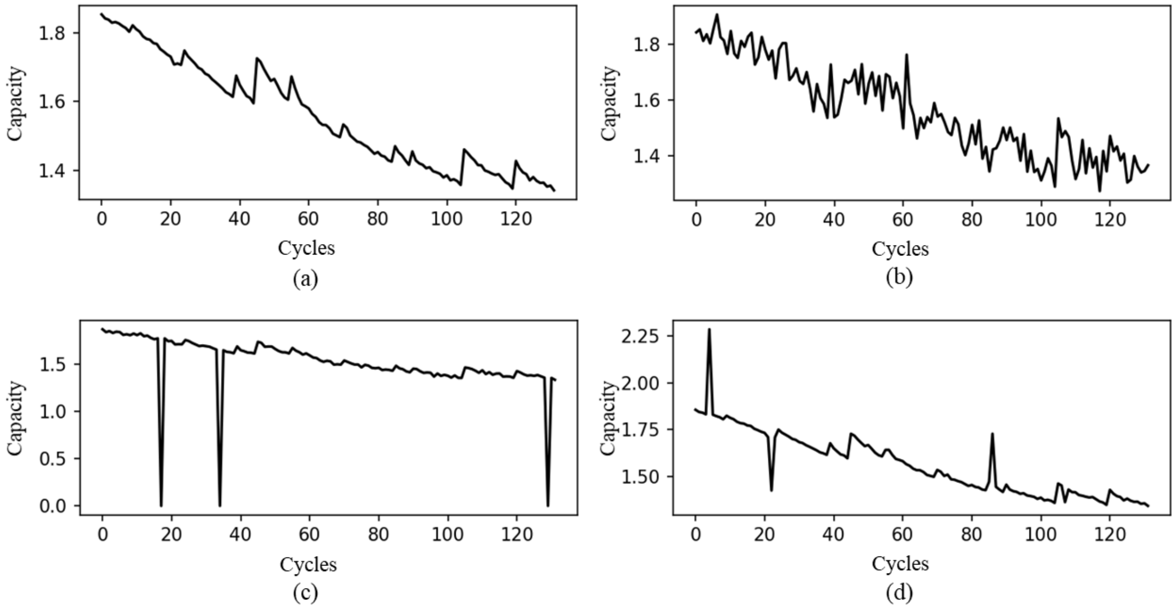

Figure 4. Analysis of original and noisy data: (a) original data without noise; (b) data with Gaussian noise, $\sigma^2 = 0.05$; (c) data with mixture noise comprising Gaussian noise with $\sigma^2 = 0.01$ and masking noise with $p = 0.03$; and (d) data with partial Gaussian noise at 2 % and $\sigma^2 = 0.05$.

first, the predictor is trained using clean data. Then, the trained model is tested using noisy data to examine its robustness. We used MSE as a loss function and evaluation metric, which is calculated in equation (2),

$$MSE = \frac{1}{N}\sum_{i=1}^{N}(x_i - \acute{x}_i)^2 \quad (2)$$

where x_i and $\acute{x}_i$ are the actual and the predicted value of the sample i, respectively.

III. Results and Discussions

A. Verification for the DAE model

We initiated our investigation by assessing the effectiveness of the DAE model. For each DAE and CNNDAE, the initial experiments were carried out with different layers depth, notated as DAE-1, DAE-2, DAE-3 for the DAE model, and CNNDAE-1, CNNDAE-2, CNNDAE-3 for CNNDAE model. The MSE of the average cross-validation results is presented in Table 3. It appears that models with only one layer, such as DAE-1 and CNNDAE-1, may be insufficient to achieve optimal performance in learning. Table 3 shows that both DAE-1 and CNNDAE-1 have higher average error values compared to their multi-layer counterparts, indicating they perform worse overall. This suggests that one-layer models might lack the complexity and capacity needed to effectively learn and generalize from the data. On the other hand, models with more layers, such as CNNDAE-2 and CNNDAE-3, demonstrate better performance. A robust denoising model is achieved using three layers of encoder and decoder networks, and CNNDAE-3 performs the best model. The capacity estimation results of DAE-2, DAE-3, CNNDAE-2, and CNNDAE-3 of batteries B5 and B18 are shown in Figure 5. From the results shown in Figures 5(a), Figure 5(e) and Figure 5(d), Figure 5(h), when there is no additional noise and slight Gaussian noise, we found that both DAE and CNNDAE can accurately predict the capacity degradation trend. However, in more considerable Gaussian noise, as in Figure 5(b) and Figure 5(f), the capacity estimated by DAE fluctuates significantly, similarly when there is a presence of mixture noise as in Figure 5(c) and Figure 5(g). As shown in Table 3, the MSE results from the CNNDAE model consistently outperformed those from the DAE model, which suggests that employing

Table 3.
MSE (mAh) of the average of cross-validation results for capacity estimation.

Model	No noise	Gaussian	Masking	Mixture	Partial Gaussian	Average
DAE-1	4.32	4.21	11.86	12.10	4.65	7.43
DAE-2	2.95	3.01	11.23	11.40	3.42	6.40
DAE-3	2.63	2.56	11.83	12.14	3.27	6.49
CNNDAE-1	5.26	6.06	6.04	6.35	6.38	6.02
CNNDAE-2	1.01	1.56	1.55	2.01	1.49	1.52
CNNDAE-3	0.36	0.92	0.42	0.93	1.06	0.74

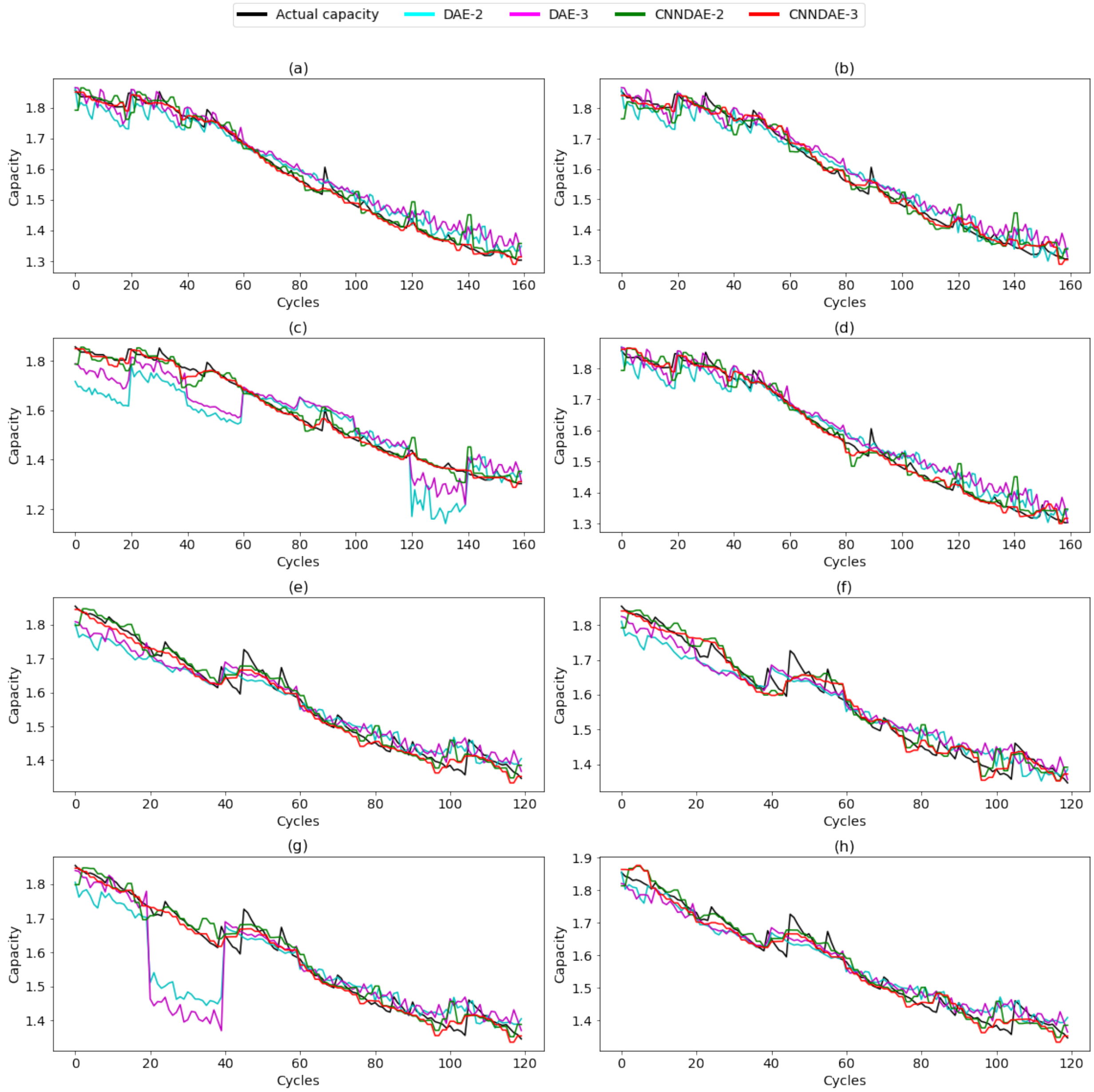

Figure 5. Capacity estimation of batteries B5 and B18 with different noise types: (a) battery B5 with no noise; (b) battery B5 with Gaussian noise, $\sigma^2 = 0.05$; (c) battery B5 with mixture noise, Gaussian noise with $\sigma^2 = 0.01$ and masking noise with $p = 0.03$; (d) battery B5 with partial Gaussian noise, 2 % with $\sigma^2 = 0.05$; (e) battery B18 with no noise; (f) battery B18 with Gaussian noise, $\sigma^2 = 0.05$; (g) battery B18 with mixture noise, Gaussian noise with $\sigma^2 = 0.01$ and masking noise with $p = 0.03$; and (h) battery B18 with partial Gaussian noise, 2 % with $\sigma^2 = 0.05$.

CNNDAE for data preprocessing leads to more accurate predictions. This is consistent with prior research indicating that convolution layers are often more effective for capturing sequential dependencies in data [32][33].

B. RUL prediction results

To further assess the effectiveness of the DAE model, the RUL prediction at a single starting point is conducted. In this experiment, we predict the RUL starts at 60 cycles. We also implemented the CEEMDAN signal analysis method as a comparison. The results for RUL prediction are summarized in Table 4, where we also included predictions without the denoising process, notated as “None” for comparison. As indicated in Table 4, when there is no noise present, the LSTM predictor can achieve accurate RUL prediction without the denoising process. The same holds for CEEMDAN, which also performs well in a noise-free environment. When the capacity data is contaminated with Gaussian noise, the performance of CEEMDAN is still comparable with CNNDAE-3. The MSE for CEEMDAN is 0.74, while for CNNDAE-3 is 0.64. This might be because CEEMDAN adopted Gaussian white noise in its denoising process. However, the performance drops significantly when masking noise is introduced. In this condition, the use of the DAE proves to be more effective than CEEMDAN.

Specifically, CNNDAE-3 stands out as the best performance among the methods evaluated. CNNDAE-3 consistently produces accurate and robust predictions compared to the others. The error rate of CNNDAE-3 is consistently below 1 mAh across all noise conditions. Even in the presence of masking noise, this predictor still ensures high prediction accuracy. The prediction results are also plotted in Figure 6,

Table 4.
MSE (mAh) of the average of cross-validation results for capacity prediction starts at 60 cycles.

Model	No Noise	Gaussian	Masking	Mixture	Partial Gaussian	Average
None	0.38	0.96	7.32	8.10	1.53	3.66
CEEMDAN	0.37	0.74	62.71	16.29	1.90	16.40
DAE-1	3.18	3.19	4.71	5.27	3.70	4.01
DAE-2	1.89	2.11	4.69	5.13	2.52	3.27
DAE-3	1.51	1.65	5.23	5.94	2.04	3.27
CNNDAE-1	2.14	3.34	2.12	2.91	3.25	2.75
CNNDAE-2	0.61	0.82	1.11	1.40	0.91	0.97
CNNDAE-3	0.38	0.64	0.37	0.82	0.85	0.61

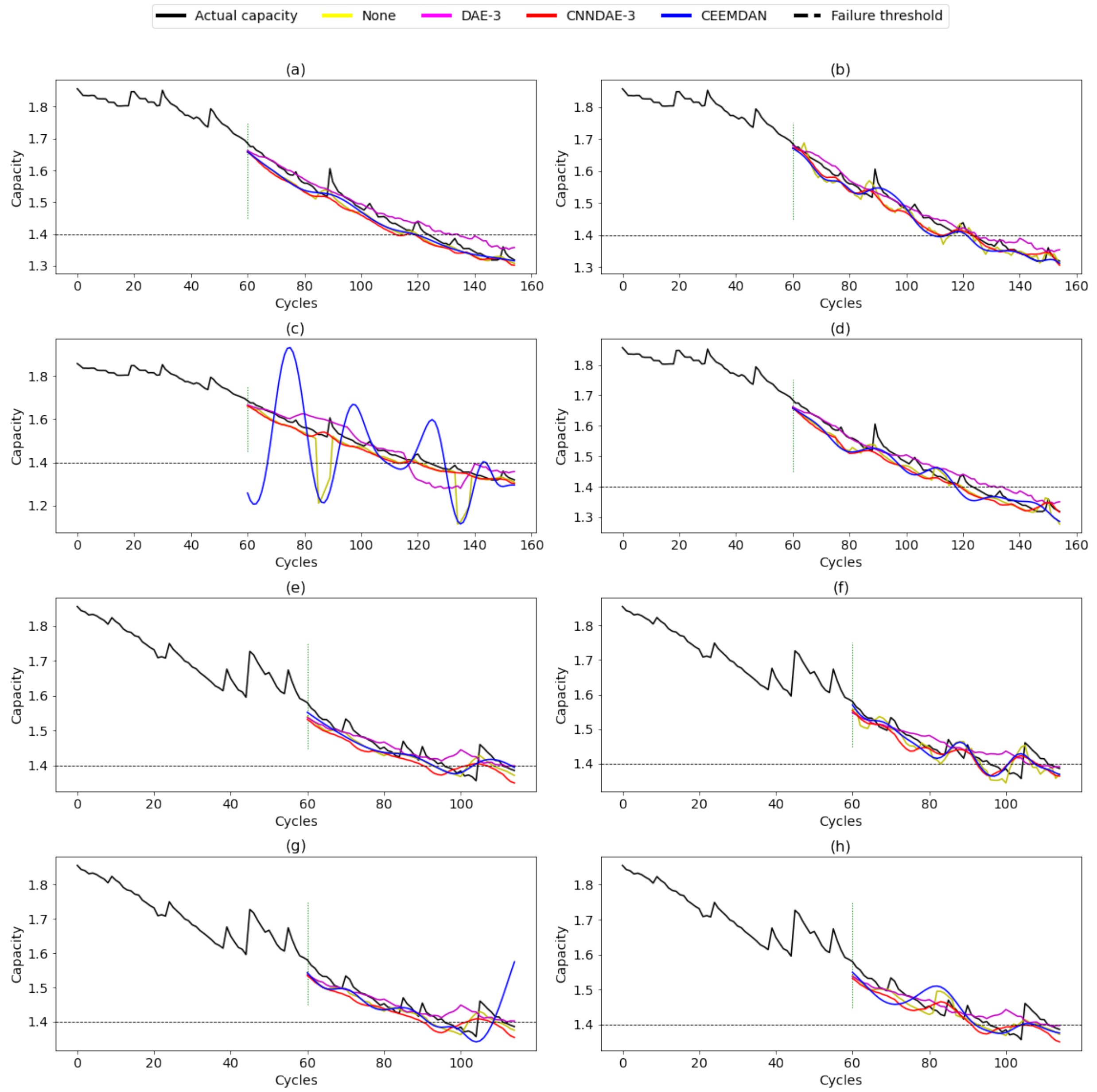

Figure 6. Capacity prediction starting at 60 cycles for batteries B5 and B18 with different noise types: (a) B5 with no noise; (b) B5 with Gaussian noise, $\sigma^2 = 0.05$; (c) B5 with mixture noise, Gaussian noise with $\sigma^2 = 0.01$ and masking noise with $p = 0.03$; (d) B5 with partial Gaussian noise at 2 % and $\sigma^2 = 0.05$; (e) B18 with no noise; (f) B18 with Gaussian noise, $\sigma^2 = 0.05$; (g) B18 with mixture noise, Gaussian noise with $\sigma^2 = 0.01$ and masking noise with $p = 0.03$; and (h) B18 with partial Gaussian noise at 2 % and $\sigma^2 = 0.05$.

Table 5.
EoL indication error: Noise type (a) no noise; (b) Gaussian noise $\sigma^2 = 0.05$; (c) mixture noise, Gaussian noise with $\sigma^2 = 0.01$ and masking noise with $p = 0.03$; and (d) partial Gaussian noise by 2 % with $\sigma^2 = 0.05$.

Model	Noise type	Actual EoL	Predicted EoL	Error
None	(a)	110	108	2
CEEMDAN			113	-3
DAE-3L			111	-1
CNNDAE-3L			106	4
None	(b)	110	120	-10
CEEMDAN			107	3
DAE-3L			108	2
CNNDAE-3L			107	3
None	(c)	110	109	1
CEEMDAN			122	-12
DAE-3L			112	-2
CNNDAE-3L			107	3
None	(d)	110	108	2
CEEMDAN			107	3
DAE-3L			111	-1
CNNDAE-3L			110	0

illustrating that CNNDAE-3 produces predictions that closely match the actual capacity values.

Finally, we investigate the EoL error of battery B18. The EoL is defined as the battery capacity exceeding the failure threshold. The failure threshold is set at 1.4 Ah, as done in [34], when the measured capacity reaches 70 % of the rated capacity. The EoL point is placed where the capacity and the failure threshold intersect, specifically at the last point of the intersection instead of the first one. In this case, the actual EoL of battery B18 is at the 110th cycle. Table 5 presents the results of EoL prediction and the associated errors for battery B18. The table illustrates that using DAE techniques (i.e. DAE and CNNDAE) to eliminate noise leads to reliable predictions, whereas comparative methods result in higher prediction errors. There is a possibility to produce inaccurate predictions when using an LSTM predictor without a denoising process or with CEEMDAN in a noisy environment.

IV. Conclusion

This paper proposes that DAE-LSTM build an accurate and robust RUL prediction in a noisy environment. Our approach involves using DAE to remove noise from the data and then utilizing an LSTM predictor to generate RUL predictions. We conducted experiments on NASA's Li-ion battery dataset to examine the effectiveness of the proposed method, where we intentionally introduced various types of artificial noise to the original capacity data. The results indicate that the proposed CNNDAE can effectively eliminate noise from the corrupted data and obtain reliable RUL prediction compared to CEEMDAN. CNNDAE has the best average performance with an MSE of 0.61 and is the most consistent model. This characteristic has the potential for practical application that demands high robustness. However, it is vital to recognize the limitations of this study for future improvements that DAE and LSTM predictors are implemented as separate tasks, and consequently, the relationship between the two tasks is not considered. Additionally, the methods are currently evaluated on artificially generated noisy data. In the future, exploration of real noisy data is needed to evaluate the effectiveness of DAE. Investigation on different types of noise, such as electrochemical noise, which is common for Li-ion battery, is also in our interest. While DAE can only learn about the latent representation of the data, using a variational autoencoder to learn about the latent distribution of the data may also improve the robustness of RUL prediction.

Declarations

Author contribution

A.R. Yuliani: Writing - Original Draft, Writing - Review & Editing, Conceptualization, Formal Analysis, Investigation, Visualization. **H.F. Pardede**: Review & Editing, Conceptualization, Supervision. **A. Ramdan**: Review & Editing, Validation, Data Curation. **V. Zilvan**: Review & Editing, Data Curation. **R.S. Yuwana**: Review & Editing. **M.F. Amri**: Review & Editing. **R.B.S.**

Kusumo: Review & Editing. **S. Pramanik**: Review & Editing.

Funding statement

This research was funded by Rumah Program Kendaraan Listrik, Research Organization for Electronics and Informatics (OREI), National Research and Innovation Agency (BRIN).

Competing interest

The authors declare that they have no known competing financial interests or personal relationships that could have appeared to influence the work reported in this paper.

Additional information

Reprints and permission: information is available at https://mev.brin.go.id/.

Publisher's Note: National Research and Innovation Agency (BRIN) remains neutral with regard to jurisdictional claims in published maps and institutional affiliations.

References

[1] J. Zhang, H. Huang, G. Zhang, Z. Dai, Y. Wen, and L. Jiang, "Cycle life studies of lithium-ion power batteries for electric vehicles: A review," *J Energy Storage*, vol. 93, p. 112231, Jul. 2024.

[2] M. Zhu, Q. Ouyang, Y. Wan, and Z. Wang, "Remaining Useful Life Prediction of Lithium-Ion Batteries: A Hybrid Approach of Grey-Markov Chain Model and Improved Gaussian Process," *IEEE J Emerg Sel Top Power Electron*, vol. 11, no. 1, pp. 143–153, Feb. 2023.

[3] S. Zhang, Q. Zhai, X. Shi, and X. Liu, "A Wiener Process Model with Dynamic Covariate for Degradation Modeling and Remaining Useful Life Prediction," *IEEE Trans Reliab*, vol. 72, no. 1, pp. 214–223, Mar. 2023.

[4] H. Feng and G. Shi, "SOH and RUL prediction of Li-ion batteries based on improved Gaussian process regression," *Journal of Power Electronics*, vol. 21, no. 12, pp. 1845–1854, Dec. 2021.

[5] R. Li, S. Zhang, P. Yang, R. Li, S. Zhang, and P. Yang, "Remaining Useful Life Estimation of Lithium-Ion Battery Based on Gaussian Mixture Ensemble Kalman Filter," *Journal of Beijing Institute of Technology*, 2022, vol. 31, no. 4, pp. 340–349, Aug. 2022.

[6] L. Zhang, Z. Mu, and C. Sun, "Remaining useful life prediction for lithium-ion batteries based on exponential model and particle filter," *IEEE Access*, vol. 6, pp. 17729–17740, Mar. 2018.

[7] M. Catelani, L. Ciani, R. Fantacci, G. Patrizi, and B. Picano, "Remaining useful life estimation for prognostics of lithium-ion batteries based on recurrent neural network," *IEEE Trans Instrum Meas*, vol. 70, pp. 1–11, Sep. 2021.

[8] X. Li, C. Yuan, and Z. Wang, "State of health estimation for Li-ion battery via partial incremental capacity analysis based on support vector regression," *Energy*, vol. 203, p. 117852, Jul. 2020.

[9] L. Cun, G. Zhengjian, and Y. Yuan, "RUL Prediction of Lithium Ion Battery Based on ARIMA Time Series Algorithm," *Materials Science Forum*, vol. 999, pp. 117–128, 2020.

[10] P. Ding *et al.*, "Useful life prediction based on wavelet packet decomposition and two-dimensional convolutional neural network for lithium-ion batteries," *Renewable and Sustainable Energy Reviews*, vol. 148, p. 111287, Sep. 2021.

[11] K. Park, Y. Choi, W. J. Choi, H.-Y. Ryu, and H. Kim, "LSTM-based battery remaining useful life prediction with multi-channel charging profiles," *IEEE Access*, vol. 8, pp. 20786–20798, Jan. 2020.

[12] A. R. Yuliani et al., "Remaining Useful Life Prediction of Lithium-Ion Battery Based on LSTM and GRU," in *The 2021 International Conference on Computer, Control, Informatics and Its Applications*, pp. 21–25, Oct. 2021.

[13] D. Gao, X. Liu, Z. Zhu, and Q. Yang, "A hybrid CNN-BiLSTM approach for remaining useful life prediction of EVs lithium-Ion battery," *Measurement and Control*, vol. 56, no. 1–2, pp. 371–383, Jan. 2023.

[14] B. Xiao, Y. Liu, and B. Xiao, "Accurate state-of-charge estimation approach for lithium-ion batteries by gated recurrent unit with ensemble optimizer," *IEEE Access*, vol. 7, pp. 54192–54202, Apr. 2019.

[15] T. Tang and H. Yuan, "A hybrid approach based on decomposition algorithm and neural network for remaining useful life prediction of lithium-ion battery," *Reliab Eng Syst Saf*, vol. 217, p. 108082, Jan. 2022.

[16] D. Chen, W. Hong, and X. Zhou, "Transformer Network for Remaining Useful Life Prediction of Lithium-Ion Batteries," *IEEE Access*, vol. 10, pp. 19621–19628, Feb. 2022.

[17] N. Gugulothu, V. Tv, P. Malhotra, L. Vig, P. Agarwal, and G. Shroff, "Predicting Remaining Useful Life using Time Series Embeddings based on Recurrent Neural Networks," *Int J Progn Health Manag*, vol. 9, no. 1, 2018.

[18] T. Qin, S. Zeng, J. Guo, and Z. Skaf, "A rest time-based prognostic framework for state of health estimation of lithium-ion batteries with regeneration phenomena," *Energies (Basel)*, vol. 9, no. 11, Nov. 2016.

[19] X. Li, L. Peng, L. Gao, D. Bi, X. Xie, and Y. Xie, "A robust hybrid filtering method for accurate battery remaining useful life prediction," *IEEE Access*, vol. 7, pp. 57843–57856, May. 2019.

[20] G. Cheng, X. Wang, and Y. He, "Remaining useful life and state of health prediction for lithium batteries based on empirical mode decomposition and a long and short memory neural network," *Energy*, vol. 232, p. 121022, Oct. 2021.

[21] J. Qu, F. Liu, Y. Ma, and J. Fan, "A neural-network-based method for RUL prediction and SOH monitoring of lithium-ion battery," *IEEE Access*, vol. 7, pp. 87178–87191, Jun. 2019.

[22] J. Chen, X. Feng, L. Jiang, and Q. Zhu, "State of charge estimation of lithium-ion battery using denoising autoencoder and gated recurrent unit recurrent neural network," *Energy*, vol. 227, p. 120451, Jul. 2021.

[23] P. Romeu, F. Zamora-Martinez, P. Botella-Rocamora, and J. Pardo, "Stacked denoising auto-encoders for short-term time series forecasting," in *Artificial Neural Networks: Methods and Applications in Bio-/Neuroinformatics*, pp. 463–486, 2015.

[24] O. M. Saad and Y. Chen, "Deep denoising autoencoder for seismic random noise attenuation," *Geophysics*, vol. 85, no. 4, pp. V367–V376, Jul. 2020.

[25] L. Ma *et al.*, "Robust state of charge estimation based on a sequence-to-sequence mapping model with process information," *J Power Sources*, vol. 474, p. 228691, Oct. 2020.

[26] C. Yu *et al.*, "Speech enhancement based on denoising autoencoder with multi-branched encoders," *IEEE/ACM Trans Audio Speech Lang Process*, vol. 28, pp. 2756–2769, Oct. 2020.

[27] P. Vincent, H. Larochelle, Y. Bengio, and P.-A. Manzagol, "Extracting and composing robust features with denoising autoencoders," in *Proceedings of the 25th International Conference on Machine Learning*, pp. 1096–1103, Jul. 2008.

[28] P. Vincent, H. Larochelle, I. Lajoie, Y. Bengio, P.-A. Manzagol, and L. Bottou, "Stacked denoising autoencoders: Learning useful representations in a deep network with a local denoising criterion," *Journal of machine learning research*, vol. 11, no. 12, Dec. 2010.

[29] Y. Bengio, Y. LeCun, and others, "Scaling learning algorithms towards AI," *Large-scale kernel machines*, vol. 34, no. 5, pp. 1–41, 2007.

[30] Y. Liu, G. Zhao, X. Peng, and C. Hu, "Lithium-ion Battery Remaining Useful Life Prediction with Long Short-term Memory Recurrent Neural Network," *Annual Conference of the PHM Society*, vol. 9, no. 1, 2017.

[31] F. K. Wang, Z. E. Amogne, J. H. Chou, and C. Tseng, "Online remaining useful life prediction of lithium-ion batteries using bidirectional long short-term memory with attention mechanism," *Energy*, vol. 254, p. 124344, Sep. 2022.

[32] M. Ma and Z. Mao, "Deep-convolution-based LSTM network for remaining useful life prediction," *IEEE Transactions on Industrial Informatics*, vol. 17, no. 3, pp. 1658-1667, May. 2020.

[33] S. Birnbaum, V. Kuleshov, S. Zayd Enam, W. Koh, and S. Ermon, "Temporal FiLM: Capturing long-range sequence dependencies with feature-wise modulations," *Advances in Neural Information Processing Systems*, 32, Dec. 2019.

[34] Y. Choi, S. Ryu, K. Park, and H. Kim, "Machine learning-based lithium-ion battery capacity estimation exploiting multi-channel charging profiles," *IEEE Access*, vol. 7, pp. 75143–75152, Jun. 2019.